Organic−Inorganic Hybrid Membrane: Thermally Stable Cation-Exchange Membrane Prepared by the Sol−Gel Method

R. K. Nagarale, G. S. Gohil, Vinod K. Shahi,* and R. Rangarajan

Central Salt & Marine Chemicals Research Institute, Bhavnagar-364002, Gujarat, India

Received August 3, 2004; Revised Manuscript Received October 4, 2004

ABSTRACT: Organic−inorganic hybrid membranes based on poly(vinyl alcohol)−SiO_2 were prepared under acidic and basic conditions, in which sulfonic acid groups were introduced at the inorganic segment. These membranes were extensively characterized for their morphology, intermolecular interactions, thermal and mechanical stability, and physicochemical properties using scanning electron microscopy (SEM), transmission electron microscopy (TEM), Fourier transform infrared (FTIR), thermogravimetric analysis (TGA), differential scanning calorimetry (DSC), dynamic mechanical analysis (DMA), and water uptake studies. Schematic models for acid-catalyzed linear weakly polymeric clusters and for base-catalyzed highly branched polymeric clusters were proposed. A higher ion-exchange capacity, permselectivity, and conductivity for the acid-catalyzed hybrid membranes than for the base-catalyzed membranes with the same composition indicated that the former route is suitable for the preparation of ion-exchange membranes. The electrochemical properties of the membrane and the equivalent pore radius were found to be highly dependent on Si content in the membrane phase. It was concluded that a definite compromise between the silica content and the membrane ion-exchange properties is required in order to have an organic−inorganic hybrid cation-exchange membrane. Furthermore, the physicochemical and electrochemical properties of these membranes were comparable to those of Nafion membrane, which suggests that they may be suitable for fuel cell and chlor-alkali applications as a substitute for Nafion membrane.

Introduction

The nanostructured organic−inorganic hybrid materials are currently the objects of intensive research, because they combine in a single solid both the attractive properties of a mechanically and thermally stable inorganic backbone and the specific chemical reactivity and flexibility of the organo-functional group. These combined properties of the hybrid nanostructured materials with diverse applications attract great attention in the fields of material science,[1−4] heterogeneous catalysis,[5,6] separation science, and fuel cells.[7−10] Most of the properties of these new materials are dependent on their structural and chemical composition as well as on the dynamic properties inside the hybrid. To develop functionalized materials/membranes, several investigators worked on the organic−inorganic hybrid materials, in which functional groups were covalently attached to the organic part of the hybrid[11−13] (such as sulfonated polysulfones, sulfonated polyetherketones, and polybenzeneimidazole). The problem with the hybrid material is that if the organic chains in these hybrids bear functional groups such as sulfonic or sulfonamide, usually they are soluble in water.[14] To decrease solubility and increase plasticity and mechanical strength, in most cases, the hybrids were cross-linked. However, very little work has been done for the applications of these materials as ion-exchange membranes, in which a functional group is attached to the inorganic part of the hybrid materials. Another choice is to disperse hybrid ion-exchangers into inorganic substrates to form supported membranes.

Several reports[15−17] are available on thio-functionalized materials, which were obtained either by grafting mercaptopropyl groups or by co-condensation of mercaptopropyltrimethoxysilane and a tetraalkoxysilane precursor for the preparation of the mesoporous materials. This mercaptopropyl group was covalently bonded with the silica framework and can be oxidized into the sulfonic acid group. However, no effort has been made to prepare organic−inorganic hybrid ion-exchange membranes using this approach. It is expected that ion-exchange membranes based on this hybrid mesoporous material may exhibit excellent thermal, mechanical, and electrochemical properties, which will arise due to the inherent properties of both components.

The main applications of poly(vinyl alcohol) (PVA) membranes are in pervaporation,[18,19] but the swelling of PVA membranes in aqueous media is a serious problem.[20,21] PVA−inorganic composites attracted our attention because such hybrids may show excellent dimensional, thermal, and mechanical stability, controllable physical properties, as well as good hydrophilic and electrochemical properties, which is essential for an ion-exchange membrane. In this paper, to control the swelling of PVA membranes and to achieve good stability, PVA−SiO_2 hybrid membranes were prepared using mercaptopropylmethyldimethoxysilane (MPDMS) and tetraethyl orthosilicate (TEOS) precursors by the sol−gel method in both acidic and basic media. The −SH group of MPDMS was oxidized to a $-SO_3H$ group by H_2O_2, to introduce a functional group in the membrane matrix. Membranes prepared by acid-catalyzed hydrolysis exhibited a high ion-exchange capacity, conductivity, and permselectivity in comparison with those prepared by base-catalyzed hydrolysis with the same composition because of the linear polymeric clusters and low cross-linking in the previous case. Furthermore, the membrane properties were found to depend on the silica content in the membrane phase.

Experimental Section

Materials. Poly(vinyl alcohol) (PVA) (M_w 125 000), hydrochloric acid, ammonia (sp gr 0.98), hydrogen peroxide (37−

* E-mail: vkshahi@csmcri.org; vinodshahi1@yahoo.com. Phone: +91-278-2569445. Fax: +91-278-2567562/2566970.

10.1021/ma048404p CCC: $27.50
Published on Web 11/23/2004

40% w/v) solution, sodium hydroxide, sodium chloride, and so forth were obtained from S. d-fine Chemicals, Mumbai, India. Tetraethyl orthosilicate (TEOS) and mercaptopropylmethyldimethoxysilane (MPDMS) were obtained from Aldrich Chemicals and used as obtained. Double-distilled water was used in all experiments.

Membrane Preparation. A 5 g portion of PVA was dissolved in 100 mL of hot deonized water in a 250 mL beaker to obtain a homogeneous solution. Then, 2 g of TEOS and 5 g of MPDMS were added while maintaining a pH of 2 in the case of the acid-catalyzed membrane and a pH of 10 in the case of the base-catalyzed membrane. The pHs of the solutions were maintained by adding 1 M HCl and 1 M NH_4OH. The resulting gel was cast on a glass plate to a desired thickness and dried at room temperature to obtain a film. These films were then immersed in a solution containing formaldehyde (54.1 g), sodium sulfate (150.0 g), sulfuric acid (125.0 g), and water (470.0 g) for 2 h at 60 °C for effecting cross-linkage in the membrane by formal reaction. The membranes obtained were subjected to oxidation for the conversion of the mecapto group into the sulfonic acid with hydrogen peroxide. The resulting membranes before being subjected to electrochemical studies were conditioned in 0.10 M HCl and 0.10 M NaOH solutions alternately several times and then equilibrated with the experimental solution for further characterization. The cation-exchange membranes (CEMs) thus prepared were designated as CEM-A/*X* for acid catalyst and CEM-B/*X* for base catalyst, where *X* is the silicon content (%) in the membrane phase.

FTIR Studies. The Fourier transform infrared (FTIR) spectra of different cation-exchange membranes were obtained using spectrum GX series 49387.

TEM and SEM Studies. The surface morphology of thoroughly dried membrane film was studied by a JEOL 1200EX transmission electron microscope. The JEOL 1200EX transmission electron microscope with a tungston electron source operates at an accelerating voltage of up to 120 kV. Images are taken directly using a built-in plate camera on the electron image film mounted at the bottom of the unit. Scanning electron microscopy (SEM) images were recorded using a Leo microscope.

Thermal and Mechanical Strength Analysis. The degradation process and the thermal stability of the membranes were investigated using thermogravimetric analysis (TGA) (Mettler Toledo TGA/SDTA851^e with star^e software) under a nitrogen atmosphere using a heating rate of 10 °C/min from 50 to 800 °C. Differential scanning calorimetry (DSC) measurements were carried out using a Mettler Toledo DSC822^e thermal analyzer with star^e software. The analysis of the mechanical strength of the membranes was carried out using a Mettler Toledo dynamic mechanical analysis (DMA) 861^e instrument with star^e software under isothermal conditions.

Ion-Exchange Capacity (IEC) and Volume Fraction of Water (φ_w) Measurements. Ion-exchange capacity was determined by equilibrating the membrane in 1.0 M HCl or 1.0 M NaOH solutions to convert the membrane into H^+ or OH^- form. The membrane was then washed free of excess HCl or NaOH with distilled water and equilibrated in it to remove the last traces of acid or base. Then, it was equilibrated in 0.10 M NaCl for 24 h and the ion-exchange capacity was determined from the increase in acidity or basicity, which in turn was determined by acid or base titration.

For the measurement of the volume fraction of water, the membrane was immersed in distilled water for 24 h and the wet membrane was weighed after mopping the surface with filter paper. This wet membrane was dried at a fixed temperature of 60 °C until a constant weight was obtained. φ_w was estimated by

$$\varphi_w = \frac{\Delta W/d_w}{\Delta W/d_w + W_d/d_m} \quad (1)$$

where ΔW is the weight difference between wet and dry membrane and d_w and d_m are the densities of water and membrane, respectively.

Membrane Potential and Conductance Studies. The experimental cell used for the membrane potential measurements[22] had two compartments separated by the membrane in circular shape with a 7.0 cm^2 area. To minimize the effect of boundary layers on potential, the solutions in both the compartments were vigorously stirred by magnetic stirrers. The potential difference developed across the membrane was recorded with the help of a multimeter (Systronics, India) using saturated calomel electrodes and salt bridges, which were reproducible up to 0.10 mV. For the membrane potential measurements, the ratio of salt concentrations on the higher to lower side (C_1/C_2) was kept constant at 9.0, while $\Delta C/C_s = 1.60$, where C_1 and C_2 are the electrolyte concentrations, $\Delta C = C_1 - C_2$, and $C_s = C_1 + C_2/2$.

The conductance measurements on the membranes were carried out separately in NaCl solutions with concentrations ranging from 0.01 to 0.06 M, using a clip type cell as reported earlier.[23] This cell is composed of two graphite electrodes fixed on plexiglass plates. The active area of the electrodes as well as the membrane was 1.0 cm^2. During the experiments, the equilibrated membrane in experimental solution was sandwiched between the electrodes and secured in place by means of a set of screws. Using the potentiostatic two-electrode mode with alternating current (ac), membrane conductance measurements were performed. Both electrodes were not in direct contact with the membrane. The membrane resistance (R^m) was estimated by subtraction of the electrolyte resistance (R_{sol}) without membrane from the membrane resistance equilibrated in electrolyte solutions (R_{cell}) ($R^m = R_{cell} - R_{sol}$). The membrane conductance was measured with the help of a digital conductivity meter (Century, model CC601, conductance range 0−200 mS, frequency 1−50 kHz, ac current) with up to ±0.01 mS reproducibility.

Electroosmotic Permeability Measurements. The electroosmotic permeability of cation-exchange membranes was measured in a two-compartment membrane cell[24] with an effective membrane area of 20.0 cm^2, in equilibration with 0.01 M NaCl solutions. Both compartments were kept in a state of constant agitation by means of magnetic and mechanical stirrers. A known potential difference was imposed across the membrane with the help of an electronically operated power supply using Ag/AgCl electrodes, and then, volumetric flux was measured by observing the movement of liquid in a horizontally fixed capillary tube of known radius. The current flowing through the system was also measured using a digital ammeter connected in series. Several measurements were performed in order to obtain reproducible values.

Results and Discussion

Membrane Preparation. The condensation polymerization of the silica precursor (mercaptopropylmethyldimethoxysilane) was carried out in aqueous media in the presence of poly(vinyl alcohol) with acid/base catalyst at room temperature for 24 h. The resulting membranes were cross-linked with formaldehyde, followed by the oxidation with hydrogen peroxide to convert the mercapto group into the sulfonic acid group; the representative reaction scheme is shown in Figure 1.

FTIR Spectroscopy. The FTIR spectra obtained for the CEM-A/50 membrane before (CEM) and after cross-linking (CEM-CL) with formaldehyde in the presence of sodium sulfate and also after the oxidation of mercapto groups to sulfonic acid groups with H_2O_2 (CEM-Ox) are presented in Figure 2. The PVA−SiO_2 hybrid membrane shows a characteristic band at 800 cm^{-1} (characteristic of the symmetric Si−O−Si stretch) and at 1100−1200 cm^{-1} (characteristic of the asymmetric Si−O−Si stretch). The presence of the −SH group was confirmed by the stretching vibration near 2600 cm^{-1}

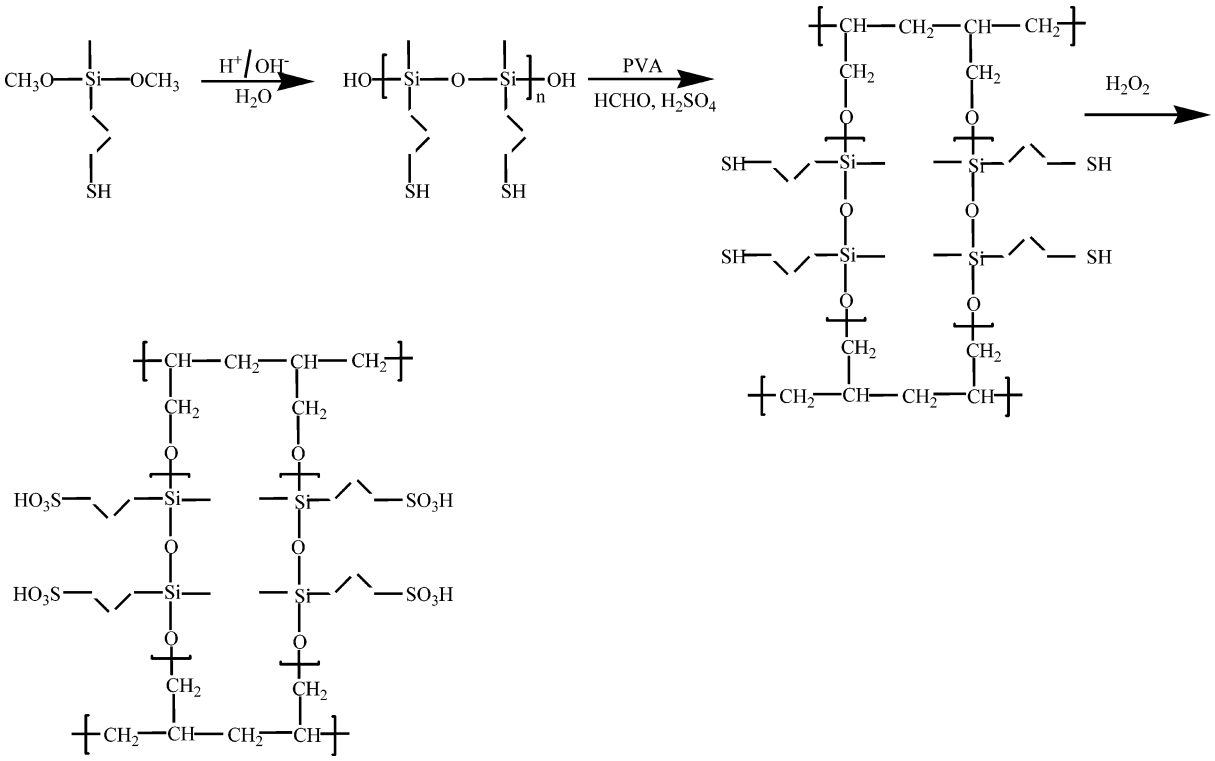

Figure 1. Reaction scheme for the membrane preparation: representative structure of the resulting membrane.

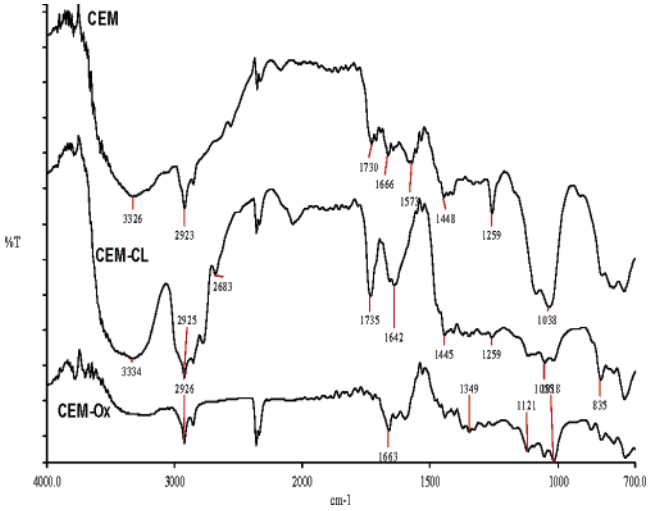

Figure 2. FTIR spectra of the acid-catalyzed membranes with 50% Si content: CEM (before cross-linking); CEM-CL (after cross-linking); CEM-Ox (after cross-linking and oxidation).

(CEM and CEM-CL), which was suppressed after the oxidation of −SH to $-SO_3H$ by H_2O_2 (CEM-Ox). Further, the presence of the broad band in the 1030−1090 cm^{-1} region confirmed SO_3H. The spectral changes clearly indicate that the hybridization between the organic and inorganic parts was successfully achieved by the sol−gel reaction. The broad peak absorption at around 3400 cm^{-1} in the hybrid membrane indicates that there was a significant number of −OH groups due to the noncondensed SiOH and/or unreacted −OH groups of the PVA. We suppose that these −OH groups provide the sites for hydrogen bonding between polymer and water, because the silica nanoparticles were observed to retain water, even at high temperatures.[25]

TEM and SEM Studies. The nature of the catalyst used for hydrolysis affects the clustering of the silica particle and thus the morphology of the resulting

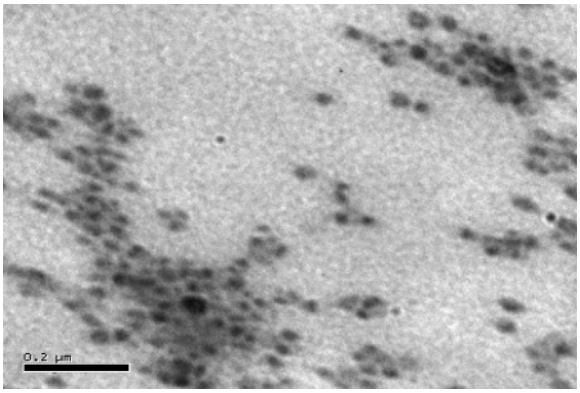

Figure 3. TEM micrograph of the CEM-B/50 membrane.

membranes.[26] Membranes prepared by condensation polymerization of silica precursors by base catalyst were less opaque in the wet state in comparison with those prepared by acid-catalyzed hydrolysis. Figure 3 shows transmission electron microscopy (TEM) images of the base-catalyzed membrane before its cross-linking. Silica clusters of nanometer sizes were observed to be dispersed in the organic matrix. Figure 4 shows SEM images for the surfaces of hybrid membranes (CEM-A/50, CEM-A/58, CEM-A/64, and CEM-A/70) with varied silica contents. The effect of silica content on the membrane morphology was clearly observed in these SEM images. With the increase in silica content in the membrane matrix, an increase in the membrane porosity was observed. Further, from all the SEM views, no phase separation of the membrane surface can be observed, suggesting that the synthesized polymeric films are homogeneous in nature and hence form dense membranes.

TGA and DSC Analysis. Thermal stability of the membranes was illustrated by the TGA and DSC analysis. The TGA curves measured under flowing nitrogen are shown in Figure 5 for CEM-A membranes

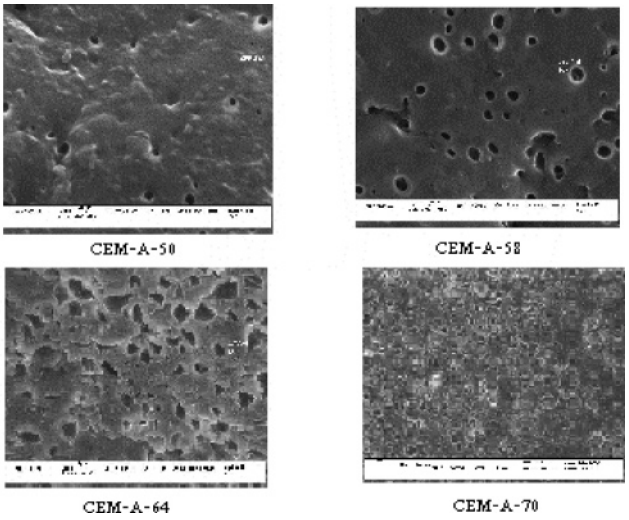

Figure 4. SEM images of the hybrid membranes with different silica contents.

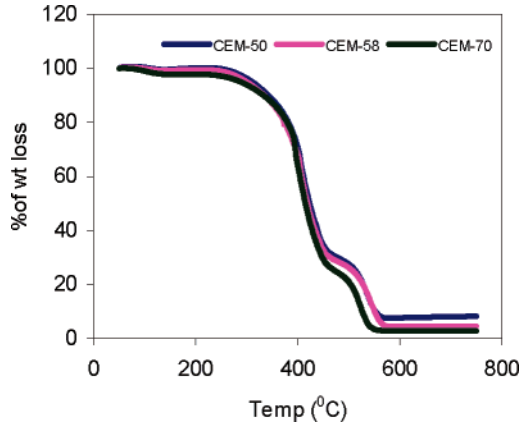

Figure 5. TGA of the acid-catalyzed hybrid membranes with different silica contents.

with a silica content of 50−70%. These curves were fitted using three main degradation stages, arising from the processes of thermal desolvation, thermal desulfonation, and thermal oxidation of the polymer matrix. The first weight loss occurred around 100 °C and was attributed to the loss of absorbed water molecules in the membrane matrix. The second weight loss region (300−400 °C) corresponds to the loss of $-SO_3H$. In the third weight loss region (at a temperature of >500 °C), the polymer residues were further degraded, which corresponds to the decomposition of the main chains of the PVA. The DSC analysis was carried out in the nitrogen atmosphere with a heating rate of 5 °C/min, and the resulting curves for the CEM-A/50 and CEM-B/50 membranes are presented in Figure 6. The acid-catalyzed membrane exhibited a T_g value around 110 °C, while the base-catalyzed membrane showed a T_g value around 120 °C. This difference in the T_g values of the membranes with a change in the catalyst may be due to the tightness of the membranes. With base catalyst, the membrane may be a bit tighter because of cross-linking of the silica clusters. These silica clusters are linear and weakly cross-linked in the membrane prepared by the acid catalyst.

DMA Studies. Figure 7 shows the representative data of mechanical strength analysis for CEM-A/50 under different applied forces ranging between 15 and 60 N at a constant temperature (100 °C) and frequency

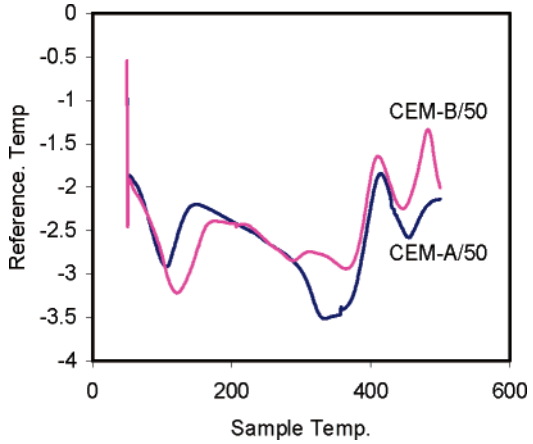

Figure 6. DSC analysis of the CEM-A/50 and CEM-B/50 hybrid membranes.

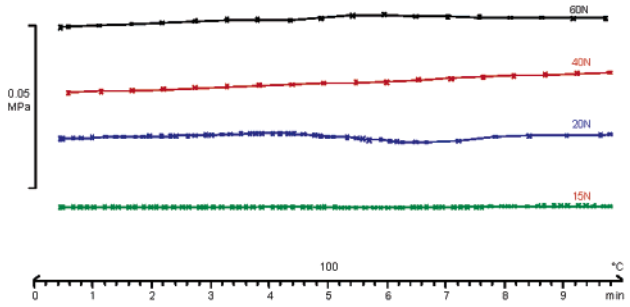

Figure 7. DMA analysis of the CEM-A-50 membrane with different forces at 100 °C and a constant frequency of 1 Hz.

(1 Hz). The membrane exhibited good mechanical stability under these experimental conditions, and no breaking of the polymeric film was observed. Dynamic mechanical curves were recorded at varying frequencies ranging between 1 and 200 Hz at a constant force (40 N) and temperature (100 °C) for acid- and base-catalyzed membranes, but the membrane seemed to be stable under these experimental conditions. It could be concluded that membranes would withstand a 60 N force at 100 °C and a 200 Hz frequency.

The organic−inorganic hybrid membranes, with molecular or nanometer level dispersion between inorganic and organic polymers by covalent or hydrogen bonding, were prepared by the sol−gel method. In these membranes, the poly(vinyl alcohol) part gives very good flexibility, while the inorganic part with sulfonic acid after oxidation of the mercapto group was responsible for good ionic conductivity with better thermal and mechanical stability. In the sol−gel process, the reaction of the silica precursor and water in the presence of acid or base forms one phase solution that goes through a solution-to-gel transition and forms a rigid two-phase system comprised of solid silica (SiO_2) and solvent-filled pores. We observed that the nature of the catalyst affects the properties of the resulting membranes. Both catalyzed reactions were bimolecular nucleophilic substitution reactions. However, the acid-catalyzed mechanisms were preceded by rapid protonation of the OR or OH substituents bonded directly to the silicon atom, whereas under basic conditions hydroxyl or silanolate anions attacked the silicon atom directly. With time, sufficient numbers of interconnected Si−O−Si bonds are

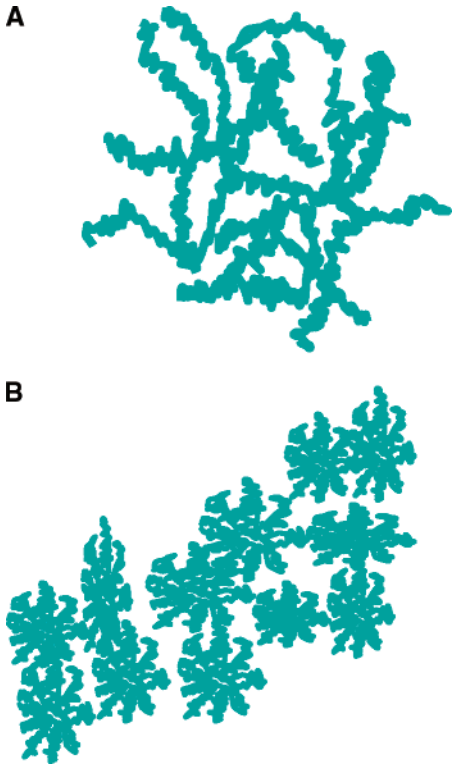

Figure 8. (A) A representative scheme for the linear weakly cross-linked polymers with acid catalyst hydrolysis. (B) A representative scheme for the highly branched clusters with base catalyst hydrolysis.

Table 1. IEC and Water Uptake Values for Different Hybrid Membranes with a 100 μm Thickness

membrane	IEC (mequiv/g)	water uptake (%)
CEM-A/50	0.865	36.25
CEM-A/58	0.987	44.57
CEM-A/64	1.106	48.97
CEM-A/70	1.210	54.83
CEM-B/50	0.613	32.19
Nafion	0.996[a]	41.00[a]

[a] Data obtained from ref 30.

formed in a region, they interact cooperatively to form colloidal particles or a sol, and further colloidal particles link together to form a three-dimensional network or a gel. Acid catalysis forms linear polymers, which are weakly cross-linked due to steric crowding, while base catalysis forms more highly branched clusters due to more rapid hydrolysis.[27] Under acidic conditions, these polymers entangle and form additional branches, resulting in gelation, and under basic conditions, gelation occurs by linking of the clusters. Representative schemes for the entanglement of linear weakly cross-linked polymers with acid catalyst hydrolysis and for the highly branched clusters with base catalyst hydrolysis are shown in parts A and B of Figure 8, respectively.

IEC and Water Uptake Properties. Ion-exchange capacity (IEC) indicates the density of ionizable hydrophilic groups in the membrane matrix, which are responsible for the ionic conductivity of the ion-exchange membrane. In general, membranes having the same degree of cross-linking and composition absorb the same amount of water, where the density of ionizable groups is the same throughout the membrane matrix.[28,29] The IEC values of all the prepared membranes are presented in Table 1. It can be seen that the IEC values ranged from 1.210 mequiv/g for CEM-A/70 to 0.865 mequiv/g for CEM-A/50. IEC values increased with an increase in the silica content on the membrane matrix. IEC arises due to the presence of the $-SO_3H$ group after the oxidation of the $-SH$ group present in MPDMS and thus is proportional to the silica content. Moreover, the IEC of CEM-A/50 is higher than that for CEM-B/50 even though they have the same composition, which may be because of the linear and low cross-linked polymer clusters in the previous case and the highly branched clusters in the latter case. For linear polymer clusters, the availability of functional groups for exchange will always be higher in comparison to highly branched polymer clusters. Further, incorporation of more silica in the membrane matrix will also lead to an increase in pore volume and thus water uptake. Thus, a definite compromise between the silica content and the membrane properties is needed.

Water uptake at equilibrium is also tabulated in Table 1 for different types of membranes. It can observed that an increase in silica content in the hybrid membrane leads to a substantial increase in water uptake of the membrane because of the increase in the density of functional groups as well as the porous volume in the membrane phase. Water uptake for the CEM-A/50 membrane was also higher than that for CEM-B/50 because of the lower degree of cross-linking compared to the previous one. Furthermore, the IEC and water uptake values of these membranes are comparable with those for Nafion membrane.[30]

Membrane Permselectivity. When electrolyte solutions of unequal concentrations are separated by a membrane, an electrical potential difference develops across the membrane due to the tendency of oppositely charged ions to move with different mobilities because of membrane permselectivity for counterions.[31,32] The magnitude of the membrane potential depends on the electrical characteristics of the membrane in addition to the nature and concentration of counterions.[33,34] Membrane potential data were obtained for different types of hybrid membranes in NaCl solutions (the mean concentration (C_s) ranged between 0.01 and 0.06 M; $C_1/C_2 = 10$ and $\Delta C/C_s = 1.60$) and were used for the estimation of membrane permselectivity. Membrane permselectivity (P_s) arises due to the nature of the ion-exchange membrane for discrimination between counterions and co-ions and can be defined by eq 2

$$P_s = \frac{t_i^m - t_i}{1 - t_i} \tag{2}$$

where t_i^m and t_i are the counterion transport numbers in the membrane phase and solution, respectively. t_i^m values under different experimental conditions were estimated from membrane potential data using the TMS (Teorell, Meyer, and Sievers) approach.[35] The permselectivity values for different acid-catalyzed organic−inorganic hybrid membranes in equilibration with sodium chloride solutions with concentrations ranging from 0.01 to 0.06 M are presented in Figure 9. Examination of the results clearly shows that membrane permselectivity decreases with equilibrating NaCl solution because of the decline in Donnan exclusion at higher electrolyte concentrations. Initially, membrane permselectivity seems to be independent of the Si content in the membrane phase. Rapid change in the membrane permselectivity was observed when varying the Si content from 60 to 65%, and afterward, it attains the limiting values in all cases. This observa-

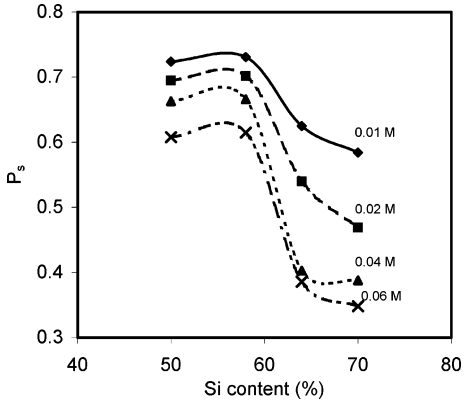

Figure 9. Variation of the permselectivity of CEM-A membranes with Si content at different concentrations of NaCl solutions.

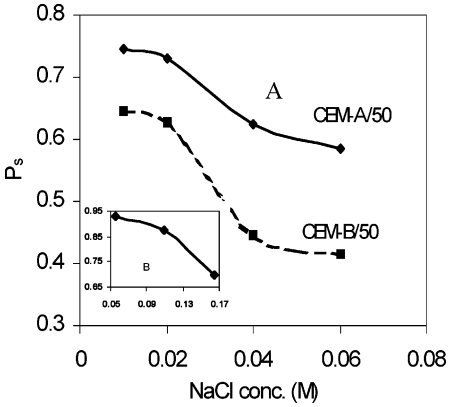

Figure 10. Dependence of membrane permselectivity on the mean concentration of NaCl solutions for (A) acid- and base-catalyzed hybrid membranes with 50% Si content and (B) Nafion membrane (ref 36).

tion may be explained by the change in pore texture of the organic−inorganic hybrid membrane with the Si content in the membrane phase. It seems void that the volume in the membrane phase increases with the incorporation of Si (which was also supported by water uptake studies and SEM images). Initially, the high density of functional groups dominated it, but at a certain Si content in the membrane phase, it was predominant and resulted in a rapid decline in Donnan exclusion and thus in lower membrane permselectivity.

At higher Si contents, membranes exhibited absolutely very low permselectivity and could not be used as ion-exchange membranes. Membrane permselectivity as a function of NaCl solution concentration was also compared between acid- and base-catalyzed membranes (CEM-A/50 and CEM-B/50) prepared with the same composition and for Nafion membrane, and the results are presented in parts A and B[36] of Figure 10, respectively. It can be seen that both types of membranes exhibited good permselectivity at lower electrolyte concentrations and the membrane permselectivity decreased at higher electrolyte concentrations. As linear polymer clusters in the case of the CEM-A membrane resulted in a high density of functional groups, it possesses a higher permselectivity in comparison with the CEM-B membrane, in which case due to the highly branched polymer clusters a low density of functional groups is present. Permselectivity values of Nafion membrane[36] were slightly higher than those of the PVA−SiO_2 hybrid membranes. Comparatively less fixed

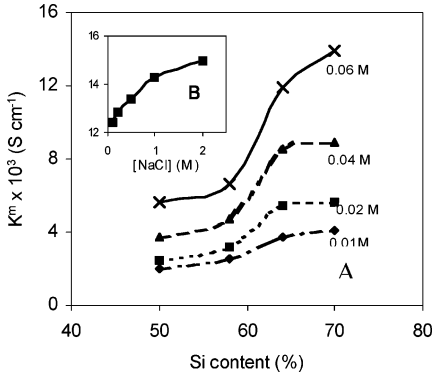

Figure 11. Variation of membrane conductivity (κ^m) with (A) Si content at different concentrations of NaCl solutions and (B) NaCl concentration for Nafion117 membrane (ref 37).

charge on the surface of the PVA−SiO_2 hybrid membranes may be responsible for the observed marginally lower permselectivity values.

Membrane Conductivity. The measurement of membrane conductivity is important for assessing the contribution of various functional groups. Membrane conductance data for different membranes with varied Si contents, equilibrated with NaCl solutions of concentrations ranging from 0.01 to 0.06 M, are presented in Figure 11A. The κ^m values increased with an increase in the equilibrating solution concentration. Also, the κ^m values initially remained constant with Si content and increased rapidly between 58 and 64% Si content before attaining a limiting value for higher Si contents. This trend in behavior is the same as that observed for water uptake and IEC behavior, which confirms the observation made on the basis of membrane permselectivity values. The membrane conductivities for acid- and base-catalyzed membranes with the same composition (CEM-A/50 and CEM-B/50) were also measured and compared. The κ^m values for the acid-catalyzed membranes were found to always be higher than those for the base-catalyzed membranes under comparable conditions probably because of the lower IEC value in the latter case. Here, we can say that the increase in the IEC value by introducing $-SO_3H$ in these hybrid membranes is not a primary factor for the increase of membrane conductivity. That is, the capacity of the membrane to contain water molecules within the polymeric structure needs to be considered seriously in any polymer design. These results suggest that the Si content with the associated IEC value should be optimized to obtain the desired membrane permselectivity and conductivity. For the purpose of comparison, the membrane conductivity values for Nafion membrane in equilibration with NaCl solutions of different concentrations[37] are also presented in Figure 11B. Under similar experimental conditions, the κ^m values for various PVA−SiO_2 hybrid membranes seem to be comparable with Nafion membrane.

Electroosmotic Studies. The electroosmotic permeability across the hybrid membranes was measured, and flux was plotted as a function of the applied current. In all the cases, a straight line was obtained. Equivalent pore radii (r) of hybrid membranes were estimated from their electroosmotic permeability values using the Katchalsky and Curran approach[38] with the help of the equation

$$r = \left(\frac{8\eta F\beta}{f^0_{1w}}\right)^{1/2} \tag{3}$$

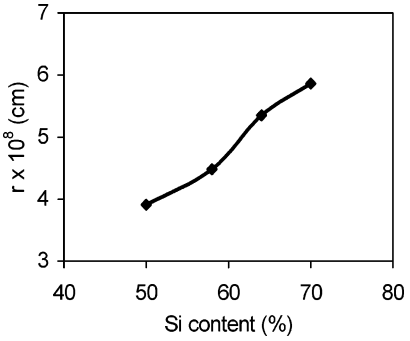

Figure 12. Variation of equivalent pore radius (r) with Si content in the membrane phase in equilibration with 0.01 M NaCl solution.

where F is the Faraday constant, β implies that every coulomb of electricity will exert a drag effect sufficient to carry β cm^3 of water through 1 cm^2 of the membrane, η denotes the coefficient of viscosity of the permeate, and f^0_{1w} is the frictional coefficient between counterion and water in free solution, which can be defined as $f^0_{1w} = RT/D_i$ (where D_i is the diffusion coefficient of the single ion i in the free solution, R is the gas constant, and T is the absolute temperature). The ionic diffusion coefficient (D_i) at a given electrolyte concentration was obtained from ionic conductance data.[39] Equivalent pore radius (r) values estimated from eq 3 for different types of hybrid membranes with varying Si contents are presented in Figure 12. r values increased with the increase in the Si content in the membrane phase. However, these values were found to be in good agreement with the equivalent capillary radius in equilibrium with 0.1 M NaCl solution (estimated by electroosmotic flux, 1.10 nm) reported by Koter[40] for Nafion 117 membranes. We also observed that the incorporation of silica in the membrane matrix leads to an increase of pore volume and consequently water uptake. An increase in pore radius leads to a reduction in Donnan exclusion and thus membrane permselectivity, and the density of functional groups depends on the MPDMS or Si content; thus, a definite compromise between the silica content and the membrane ion-exchange properties is essential in order to have an organic−inorganic hybrid cation-exchange membrane with the desired properties.

Conclusions

Organic−inorganic hybrid membranes based on PVA−SiO_2 hybrids, in which $-SO_3H$ groups are introduced by oxidation of the existing −SH group in MPDMS, were prepared using a sol−gel process under acidic and basic conditions, and their physicochemical and electrochemical properties have been studied. This is a relatively new method where functional groups were introduced in the preformed hybrid film by the oxidation of the −SH group in the presence of H_2O_2 and leads to the formation of a homogeneous type of cation-exchange membrane. It was found that the membrane properties depend on the nature of conditions under which they were prepared. Under acidic conditions, linear polymeric clusters were formed, which are weakly cross-linked, while, under basic conditions, highly branched polymeric clusters were formed due to more rapid hydrolysis. Hybrid membranes prepared under acidic conditions have advantages over those prepared under basic conditions because of their high IEC, permselectivity, and conductivity values.

Characterization by TGA, DSC, and DMA testing revealed an adequate thermal and mechanical stability of the membrane, which is essential for thermally stable cation-exchange membranes. These membranes with high water uptake, moderate IEC values, good ionic conductivity, and good permselectivity with no significant effect on thermal and mechanical stability offer a new dimension for the preparation of organic−inorganic hybrid membranes, in which the membrane porosity and density of functional groups could be controlled by the inorganic content. Different electrochemical properties of these membranes were compared with those of Nafion membrane and were found to be in good agreement. Furthermore, with improved physicochemical and electrochemical properties, these membranes will be suitable for fuel cell and chlor-alkali applications as a substitute for Nafion membrane.

Acknowledgment. The authors are grateful to Dr. P. K. Ghosh, Director, CSMCRI, Bhavnagar, for his keen interest and encouragement. Financial assistance from DST, Govt. of India, for funding project no. SR/S1/PC-15/2003 is also gratefully acknowledged. Help rendered by the analytical section of this institute for FTIR, TGA, DSC, DMA, and SEM analysis is also gratefully acknowledged.

References and Notes

(1) Ganesan, V.; Walcarius, A. *Langmuir* **2004**, *20*, 3632.
(2) Percy, M. J.; Michailidou, V.; Armes, S. P.; Perruchot, C.; Watts, J. F.; Greaves, S. J. *Langmuir* **2003**, *19*, 2072.
(3) Matejka, L.; Dukh, O.; Meissner, B.; Hlavata, D.; Brus, J.; Stachota, A. *Macromolecules* **2003**, *36*, 7977.
(4) Bhaumik, A.; Inagaki, S. *J. Am. Chem. Soc*. **2001**, *123*, 691.
(5) Corma, A. *Top. Catal*. **1998**, *4*, 249.
(6) De Vos, D. E.; Dams, M.; Sels, B. F.; Jacobs, P. A. *Chem. Rev*. **2002**, *102*, 3615.
(7) Sforca, M. L.; Yoshida, I. V. P.; Nunes, S. P. *J. Membr. Sci*. **1999**, *159*, 197.
(8) Yong-il, P.; Masayuki, N. *Solid State Ionics* **2001**, *145*, 149.
(9) Kerres, J. A. *J. Membr. Sci*. **2001**, *185*, 3.
(10) Luneau, G. I.; Denoyelle, A.; Sanchez, J. Y. *Trochimica Acta* **1992**, *37* (9), 1615.
(11) Yunsong Yang, Z.; Steven, H. *Macromolecules* **2004**, *37*, 1678.
(12) Smitha, B.; Sridhar, S.; Khan, A. A. *Macromolecules* **2004**, *37*, 2233.
(13) Genova-Dimitrova, P.; Baradie, D. F.; Poinsignon, C.; Sanchez, J. Y. *J. Membr. Sci*. **2001**, *185*, 59.
(14) Wu, C.; Xu, T.; Yang, W. *J. Membr. Sci*. **2003**, *224*, 117.
(15) Lim, M. H.; Blanford, C. F.; Stein, A. *Chem. Mater.* **1998**, *10*, 467.
(16) Margolese, D.; Melero, J. A.; Christiansen, S. C.; Chmelka, B. F.; Stucky, G. D. *Chem. Mater*, **2000**, *12*, 2448.
(17) Shen, J. G. C.; Herman, R. G.; Klier, K. *J. Phys. Chem. B* **2002**, *106*, 9975.
(18) Rhim, J. W.; Lee, S. W.; Kim, Y. K. *J. Appl. Polym. Sci.* **2002**, *85*, 1867.
(19) Rhim, J. W.; Kim, Y. K. *J. Appl. Polym. Sci.* **2000**, *75*, 1699.
(20) Uragami, T.; Okazaki, K.; Matsugi, H.; Miyata, T. *Macromolecules* **2002**, *35*, 9156.
(21) Mallapragada, S. K.; Peppas, N. A. *J. Polym. Sci., Part B: Polym. Phys.* **1996**, *34*, 1339.
(22) Nagarale, R. K.; Shahi, V. K.; Schubert, R.; Rangarajan, R.; Mehnert, R. *J. Colloid Interface Sci*. **2004**, *270*, 446.
(23) Nagarale, R. K.; Gohil, G. S.; Shahi, V. K.; Trivedi, G. S.; Rangarajan, R. *J. Colloid Interface Sci*. **2004**, *277*, 162.
(24) Shahi, V. K.; Trivedi, G. S.; Thampy, S. K.; Rangarajan, R. *J. Colloid Interface Sci*. **2003**, *262*, 566.
(25) Nogami, M.; Nagao, R.; Wong, C. *J. Phys. Chem. B* **1998**, *102*, 5772.
(26) Hench, L. L.; West, J. *Chem. Rev*. **1990**, *90*, 33.
(27) Klemperer, W. G.; Mainz, V. V.; Ramamurthi, S. D. In *Better Ceramics Through Chemistry III*; Brinker, C. J., Clark, D. E., Ulrich, D. R., Eds.; Materials Research Society: Pittsburgh, PA, 1988; Vol. 121, p 15.

(28) Shahi, V. K.; Thampy, S. K.; Rangarajan, R. *React. Funct. Polym*. **2000**, *46*, 39.
(29) Koter, S.; Piotrowski, P.; Kerrs, J. *J. Membr. Sci*. **1999**, *153*, 83.
(30) Yang, C.; Srinivasan, S.; Bocarsly, A. B.; Tulyani, S.; Benziger, J. B. *J. Membr. Sci*. **2004**, *237*, 145.
(31) Singh, K.; Shahi, V. K. *J. Membr. Sci*. **1990**, *59*, 27.
(32) Yamauchi, A.; Shiozaki, M.; Shin, Y.; Kawake, M. *J. Membr. Sci*. **1999**, *163*, 289.
(33) Singh, K.; Tiwari, A. K. *J. Colloid Interface Sci*. **1999**, *210*, 241.
(34) Shahi, V. K.; Thampy, S. K.; Rangarajan, R. *J. Membr. Sci*. **1999**, *158*, 77.
(35) Lakshiminarayanaiah, N. *Transport Phenomena in Membranes*; Academic Press: New York, 1969.
(36) Singh, K.; Shahi, V. K. *J. Membr. Sci*. **1998**, *140*, 51.
(37) Lehmani, A.; Turq, P.; Perie, M.; Perie, J.; Simonin, J.-P. *J. Electranal. Chem.* **1997**, *428*, 81.
(38) Katchalsky, A.; Curran, P. F. *Nonequilibrium Thermodynamics in Bionphysics*; Harvard University Press: Cambridge, MA, 1965.
(39) Parsons, R. *Handbook of Electrochemical Constants*; Butterworths: London, 1959.
(40) Koter, S. *J. Membr. Sci*. **2000**, *166*, 127.

MA048404P